# Biogeochemical and plant trait mechanisms drive enhanced methane emissions in response to whole-ecosystem warming

Genevieve L. Noyce and J. Patrick Megonigal

Smithsonian Environmental Research Center, Edgewater, MD

Corresponding author: G. Noyce, noyceg@si.edu, 443-482-2351

**Abstract**

Climate warming perturbs ecosystem carbon (C) cycling, causing both positive and negative feedbacks on greenhouse gas emissions. In 2016, we began a tidal marsh field experiment in two vegetation communities to investigate the mechanisms by which whole-ecosystem warming alters C gain, via plant-driven sequestration in soils, and C loss, primarily via methane ($CH_4$) emissions. Here, we report the results from the first four years. As expected, warming of 5.1 °C more than doubled $CH_4$ emissions in both plant communities. We propose this was caused by a combination of four mechanisms: (i) a decrease in the proportion of $CH_4$ consumed by $CH_4$ oxidation, (ii) more C substrates available for methanogenesis, (iii) reduced competition between methanogens and sulfate reducing bacteria, and (iv) indirect effects of plant traits. Plots dominated by *Spartina patens* consistently emitted more $CH_4$ than plots dominated by *Schoenoplectus americanus*, indicating key differences in the roles these common wetland plants play in affecting anerobic soil biogeochemistry and suggesting that plant composition can modulate coastal wetland responses to climate change.

## 1. Introduction

Methane ($CH_4$) is a potent greenhouse gas that contributes to 15-19 % of total greenhouse gas radiative forcing (IPCC, 2013) and has a sustained-flux global warming potential that is 45 times that of $CO_2$ on a 100-year timescale (Neubauer & Megonigal, 2015). Wetlands are the largest natural source of $CH_4$ to the atmosphere and were recently identified as the largest source of uncertainty in the global $CH_4$ budget (Saunois et al., 2016). Recent estimates calculate that $CH_4$ emissions from vegetated coastal wetlands offset 3.6 of the 12.2 million metric tons (MMT) of $CO_2$ equivalents accumulated by these ecosystems each year (EPA, 2017). Despite this, there is still a substantial knowledge gap regarding how global change factors, such as climate warming, will alter coastal wetland $CH_4$ emissions (Mcleod et al., 2011) even though these feedbacks have the potential to shift coastal wetlands from being a net sink of C to a net source (Al-Haj & Fulweiler, 2020; Bridgham et al., 2006).

The net flux of $CH_4$ to the atmosphere from any ecosystem represents the balance between the amount of $CH_4$ produced (methanogenesis), the amount of $CH_4$ oxidized (methanotrophy), and the rate of $CH_4$ transport from the soil. In coastal wetlands, methanogenesis occurs through three pathways: (i) hydrogenotrophic methanogenesis (i.e. $CO_2$ reduction) in which $H_2$ is the electron donor and $CO_2$ is the electron acceptor, (ii) acetoclastic methanogenesis, in which acetate ($CH_4COOH$) is split into $CH_4$ and $CO_2$ and (iii) methylotrophic methanogenesis in which methylated compounds are converted to $CH_4$ and $CO_2$ (Conrad, 2020; Oremland et al., 1982; Schlesinger & Bernhardt, 2020). Rates of methanogenesis are driven by low redox conditions and substrate availability, while aerobic $CH_4$ oxidation requires both $O_2$ and $CH_4$ as substrates. Roots and rhizomes in wetland ecosystems influence methane-related substrates through at least two mechanisms: (i) deposition of organic compounds that support multiple pathways of heterotrophic microbial respiration, including methanogenesis, and (ii) release of $O_2$ that simultaneously promotes $CH_4$ oxidation and regeneration of competing electron acceptors such as Fe(III) and $SO_4$ (Philippot et al., 2009; Stanley & Ward, 2010). Root exudates, which typically include low-molecular-weight compounds, may either be more readily used by microbes than existing soil C (Kayranli et al., 2010; Megonigal et al., 1999) or may prime microbial use of soil C (Basiliko et al., 2012; Philippot et al., 2009; Robroek et al., 2016; Waldo et al., 2019). Root exudates can also decrease $CH_4$ oxidation by stimulating use of $O_2$ by other aerobic microbes (Lenzewski et al., 2018; Mueller et al., 2016). Consequently, wetland $CH_4$ emissions are strongly linked to a wide variety of plant traits that govern the supply of reductive (organic carbon) and oxidative ($O_2$) substrates to soils (Moor et al., 2017; Mueller et al., 2020).

Although it is understood that wetland plants are a primary control on $CH_4$ emissions and that much of their influence is mediated through conditions in the rhizosphere (Waldo et al., 2019), there are surprisingly few data, especially from coastal wetlands, that couple plant responses to the dynamics of electron donors (organic C), electron acceptors ($O_2$, $SO_4$), and the rates of competing (sulfate reduction vs methanogenesis) or opposing ($CH_4$ production vs $CH_4$ oxidation) microbial processes. The general lack of process data on wetland $CH_4$ cycling makes it difficult to forecast ecosystem responses to climate change.

For example, the well-documented observation that warming increases wetland methane emissions can be either amplified or dampened depending on changes in plant activity (e.g. primary production) or plant traits (e.g. community composition) (Mueller et al., 2020). Vegetation composition has been shown to be a stronger control on $CH_4$ emissions than ~1 °C of warming in northern peatlands (Ward et al., 2013) and Chen et al. (2017) proposed that warming effects on plant functional types can drive C flux responses that cannot otherwise be explained by abiotic conditions. In freshwater marshes, plant species and growth trends have also been linked to seasonal shifts in pools of dissolved $CH_4$ and DIC (Ding et al., 2005; Stanley & Ward, 2010) and methanogenesis dynamics (Sorrell et al., 1997).

Tidal wetlands are particularly good model systems for determining the mechanisms by which warming alters $CH_4$ emissions. Not only will the $CH_4$ cycle respond to the direct effects of warming, but the temperature effects on the outcome of competition for electron acceptors is relatively easily observed because of the abundance of $SO_4$. Thermodynamic theory in which terminal electron acceptors (TEAs) are used in order of decreasing thermodynamic yield is commonly interpreted to mean that a system will support only one form of anaerobic respiration at time, with acetoclastic and hydrogenotrophic methanogenesis occurring only when pools of more energetically favorable TEAs have been depleted (Conrad, 2020; Schlesinger & Bernhardt, 2020). However, in real systems with spatial and temporal variability in the supply of electron donor substrates and TEAs, all forms of anaerobic metabolism occur simultaneously (Megonigal et al. 2004, Bridgham et al., 2013). Much of this spatial and temporal variation arises from the distribution and activity of roots and rhizomes as mediated by the rhizosphere (Neubauer et al., 2008). Global change factors such as warming will further affect the spatial distribution of key metabolic substrates. In addition, the relatively-limited species diversity in saline tidal wetlands allows species-level effects on $CH_4$ cycling to be delineated more easily than in diverse freshwater wetlands.

Methane flux measurements are a metric of broader shifts in redox potential and biogeochemical cycling, as they are sensitive to virtually all processes that regulate availability of electron donors and electron acceptors. Emissions are commonly predicted to increase with future climate warming, including

from coastal wetlands (Al-Haj & Fulweiler, 2020), but there is minimal prior understanding of the underlying mechanisms, which was the focus of this study. Our objectives were to explore the mechanisms that drive enhanced $CH_4$ emissions under warming. To accomplish this, we measured monthly $CH_4$ emissions from 2016 through 2019 and coupled these flux measurements with analysis of porewater biogeochemistry and vegetation biomass and composition.

## 2. Materials and Methods

### 2.1 Site Description and Experimental Design

The Salt Marsh Accretion Response to Temperature eXperiment (SMARTX) was established in the Smithsonian's Global Change Research Wetland (GCReW) in 2016. GCReW is part of Kirkpatrick Marsh, a microtidal, brackish high marsh on the western shore of the Chesapeake Bay, USA (38°53' N, 76°33' W). Soils are organic (>80 % organic matter) to a depth of 5 m, which is typical of high marshes in the Chesapeake Bay and elsewhere. The very low mineral content (<20%) affects methane dynamics because negligible competition between methanogens and iron-reducing bacteria for electron donors is expected in the absence of a significant pool poorly crystalline iron oxides (Roden & Wetzel, 1996), as has been documented previously at this site (Weiss et al., 2004) (Weiss et al. 2004). Soil bulk density in the upper 60 cm averages 0.124 g $cm^3$ and ranges from 0.079 to 0.180 g $cm^3$. The relatively uniform bulk density of the soil profile reflects the uniform soil organic matter content and the fact that bulk density becomes largely independent of organic matter and mineral content once organic matter content exceeds 50% (Holmquist et al., 2018). The marsh is typically saturated to within 5-15 cm of the soil surface, but inundation frequency varies across the site, from 10-20 % of high tides in high elevation areas to 30-60 % of high tides in low elevation areas.

SMARTX consists of six replicate transects, three located in each of the two dominant annual plant communities (Fig. S1). In the $C_3$-dominated community (herein the '$C_3$ community') the $C_3$ sedge *Schoenoplectus americanus* (herein *Schoenoplectus*) composes more than 90 % of the aboveground biomass (Table 1). In the $C_4$-dominated community (herein the '$C_4$ community'), 75 % of the

aboveground biomass was initially composed of two $C_4$ grasses (*Spartina patens* and *Distichlis spicata*, herein *Spartina* and *Distichlis*, respectively). However, by 2019, *Spartina* and *Distichlis* declined to 56 % of the aboveground biomass (Table 1).

Table 1. Relative contribution to total aboveground biomass from $C_3$ sedges (*Schoenoplectus americanus*) and $C_4$ grasses (*Spartina patens* and *Distichlis spicata*) in each plant community. Values are means and SE (n = 12).

| | $C_3$ community | | $C_4$ community | |
|---|---|---|---|---|
| Year | % $C_3$ | % $C_4$ | % $C_3$ | % $C_4$ |
| 2016 | 93 (3) | 8 (3) | 8 (2) | 76 (6) |
| 2017 | 91 (3) | 9 (3) | 10 (3) | 64 (4) |
| 2018 | 95 (1) | 5 (1) | 15 (4) | 65 (7) |
| 2019 | 93 (2) | 4 (1) | 23 (5) | 56 (6) |

Each transect is an active warming gradient consisting of unheated ambient plots and plots that are heated to 1.7 °C, 3.4 °C, and 5.1 °C above ambient. All plots are 2 x 2 meters with a 20 cm-wide buffer around the perimeter. Aboveground plant-surface temperature is elevated via infrared heaters and soil temperature is elevated via vertical resistance cables (Rich et al., 2015). Soils are heated to a depth of 1.5 m, which is the depth most vulnerable to climate or human disturbance (Pendleton et al., 2012). Aboveground and belowground temperature variation are assessed via thermocouples embedded in acrylic plates at plant canopy level and inserted into the soil, respectively, and the temperature gradient is maintained by integrated microprocessor-based feedback control (Rich et al., 2015). Noyce et al. (2019) provides additional details of the heating system. Warming began on 1 Jun 2016 and has continued year-round.

## 2.2 Methane flux measurements

Methane emissions were measured monthly year-round from May 2016 to Dec 2019 using a static chamber system. One permanent 160 $cm^2$ aluminum base was inserted 10 cm into the soil in each plot in Apr 2016. On each measurement date, clear chambers (40 x 40 x 40 cm) were gently placed on top of each base and secured with compression clips. Chambers consisted of an aluminum frame with transparent sides made of polychlorotrifluoroethylene film (Honeywell International) and closed-cell foam on the base. Depending on the height of the vegetation at the time of measurement, chambers were stacked up to four high (total height of 40 to 160 cm) (Fig. S2). The advantage of this stacking method is

that it uses the minimal chamber volume necessary, while also allowing for plant growth. After placement, the chambers were left open for at least 10 minutes, to minimize disturbance effects and allow air inside the chamber to return to ambient conditions. During data collection, chambers were covered with a transparent polycarbonate top equipped with sampling tubes, a fan to circulate air inside the chambers, a PAR sensor, and thermocouples. The sealed chamber was covered with a foil shroud to block out all light and to minimize changes in temperature and relative humidity during the measurement period. An UltraPortable Greenhouse Gas Analyzer (Los Gatos Research, CA) was used to measure headspace $CH_4$ concentrations for 5 min. Plots were accessed from permanent boardwalks elevated 15 cm above the soil surface to avoid compressing the surrounding peat and altering diffusive $CH_4$ emissions. Fluxes were calculated as the slope of the linear regression of $CH_4$ concentration over time. The 40 fluxes where $p > 0.05$ were assigned a value of ½ the limit of detection of the system (Wassmann et al., 2018; Table S1). This was 1 % of fluxes during the growing season and 4.5 % of fluxes over the remaining months. For 2017-2019, monthly measurements were scaled to annual estimates by regressing $CH_4$ emissions against daily mean soil temperature and day of year (as a proxy for phenological status). Annual estimates were not calculated for 2016 because flux measurements did not start until May.

2.3 Porewater sampling and analysis

Porewater samples were collected in May, Jul, and Sep of each year using stainless steel ‘sippers’ permanently installed in each plot. Each sipper consisted of a length of stainless-steel tubing, crimped and sealed at the end, with several slits (approximate width 0.8 mm) cut in the bottom 2 cm. The aboveground portion of each sipper was connected to Tygon Masterflex® tubing capped with a 2-way stopcock. In May 2016, duplicate clusters of sippers were installed in each of the 30 plots at 20, 40, 80, and 120 cm below the soil surface. An additional set of 10 cm-deep sippers was installed in 2017. In this study we defined samples from 10-20 cm as “rooting zone” samples and samples from 40-120 cm as "deep peat" samples. On sampling dates, porewater sitting in the sippers was drawn up and discarded, after which 60 mL of porewater from each depth (30 mL from each sipper) was withdrawn and stored in syringes equipped with 3-way stopcocks. A 10 mL-aliquot of each sample was filtered through a pre-leached 0.45

177 µm syringe-mounted filter, preserved with 5 % zinc acetate and sodium hydroxide, and frozen for future
178 $SO_4$ and Cl analysis. Dissolved $CH_4$ was extracted from 15 mL of porewater in the syringe by drawing 15
179 mL of ambient air and shaking vigorously for 2 min to allow the dissolved $CH_4$ to equilibrate with the
180 headspace. Headspace subsamples were then immediately analyzed on a Shimadzu GC-14A gas
181 chromatograph equipped with a flame ionization detector. 3 mL of porewater was used to measure pH
182 using a Fisher Scientific accumet electrode (13-620-290). The remaining porewater was used to measure
183 $H_2S$, and $NH_4$; those data are not reported here.
184 $SO_4$ and Cl were measured on a Dionex ICS-2000 ion chromatography system (2016-2018) or a
185 Dionex Integrion (2019). On the Dionex ICS-2000 samples were separated using an A11 column with 30
186 mM of KOH as eluent; on the Dionex Integrion samples were separated using an A11-4µm-fast column
187 with 35 mM KOH. Sulfate depletion ($Sulfate_{Dep}$) was calculated based on measured porewater
188 concentrations of $SO_4$ ($SO_{4pw}$) and Cl ($Cl_{pw}$) and the constant molar ratio of Cl to $SO_4$ in surface seawater
189 ($R_{sw}$ = 19.33; Bianchi, 2006) using the following equation: $Sulfate_{Dep} = Cl_{pw} / R_{sw} - SO_{4pw}$. If driven only
190 by seawater inputs, the ratio of Cl to $SO_4$ would remain constant, but under anaerobic conditions $SO_4$ can
191 be reduced by sulfate reducing bacteria, altering this ratio. As a result, $SO_4$ depletion can be used as a
192 proxy for $SO_4$ reduction rates.
193 2.4 Plant biomass measurements
194 Measurements of *Schoenoplectus*, *Spartina*, and *Distichlis* biomass were conducted during peak
195 biomass of each year (29 Jul – 2 Aug) as described by Noyce et al. (2019). *Schoenoplectus* biomass was
196 estimated using non-destructive allometric techniques (Lu et al., 2016) in 900-$cm^2$ quadrats, and *Spartina*
197 and *Distichlis* biomass were estimated through destructive harvest of 25-$cm^2$ subplots.
198 2.5 Data analysis
199 Statistics were conducted in R (version 3.6.3). Methane flux (Fig. S3) and porewater data were log
200 transformed to become normally distributed prior to statistical analyses. The 'growing season' was
201 defined as May through Sep based on *Schoenoplectus* growth trends (Fig. S4). Pearson's correlations
202 were used to test the relationships between $CH_4$ flux and soil temperature, and $CH_4$ flux and plant

biomass. Responses of $CH_4$ emissions to vegetation type and warming treatment were analyzed using linear mixed models with vegetation community and warming treatment as categorial variables, and plot and year as random effects. P-values were calculated using Satterthwaite's method and Tukey's post-hoc tests were used to compare individual means. Porewater data was averaged per year and then analyzed using one-way ANOVAs to determine the effects of warming treatment or plant community, applying Tukey's HSD test for post-hoc analyses.

## 3. Results

### 3.1 Environmental conditions, site characteristics, and experiment performance

The growing season of 2016 was the hottest of the four years, with growing season temperatures averaging >1 °C above the other three years (Table 2). While 2017 through 2019 had similar summer temperatures, they had very different precipitation regimes; 2018 was much wetter on average and 2019 was slightly drier (Table 2). During all years, temperatures in the experimental plots were successfully shifted by the target differentials of +1.7, +3.4, and +5.1 °C above the ambient plots (Fig. 1; Noyce et al., 2019). Porewater pH ranged from 6.4 to 6.8 across the measurement period, with no effect of temperature treatment ($p > 0.1$; data not shown). There was no difference in soil bulk density between the ambient and +5.1 °C plots after 4.5 years of warming ($p = 0.54$; data not shown).

Table 2. Growing season (May-Sep) temperature and precipitation. Temperature data are means (SE) of daily averages from ambient plots and precipitation is total from May through September.

| Year | Mean aboveground temperature (°C) | Mean soil temperature (°C) | Total precipitation (cm) |
|---|---|---|---|
| 2016 | 24.7 (0.3) | 22.4 (0.2) | 51.0 |
| 2017 | 22.0 (0.3) | 20.7 (0.2) | 51.1 |
| 2018 | 23.7 (0.3) | 20.8 (0.2) | 86.4 |
| 2019 | 23.6 (0.3) | 20.9 (0.2) | 43.7 |

### 3.2 Methane fluxes

Methane emissions increased with soil temperature ($R^2 = 0.41$, $p < 0.001$) (Fig. 1). Emissions from all treatments had strong seasonal trends; fluxes were highest in the $C_3$ community in Jun through Aug

and peak fluxes in the $C_4$ community were shifted about a month later to Jul through Sep (Fig. S3). Whole-ecosystem warming increased $CH_4$ emissions throughout the growing season ($F_{3,400}$ = 5.1, $p$ = 0.002; Fig. 2). Across all four years, 5.1 °C of warming more than doubled growing season emissions, from 624 to 1413 µmol $CH_4$ $m^{-2}$ d ($p_{adj}$ = 0.02; Fig. 2).

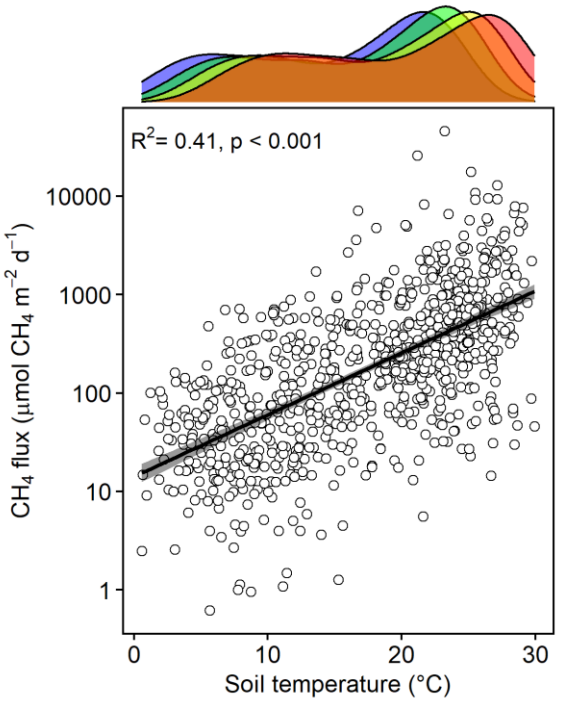


Figure 1. Bottom: $CH_4$ emissions from each plot versus the soil temperature at the time of measurement. Top: Density plot depicting the range of soil temperatures in each treatment, delineated by color: ambient (blue), +1.7°C (green), +3.4°C (yellow), +5.1°C (red).

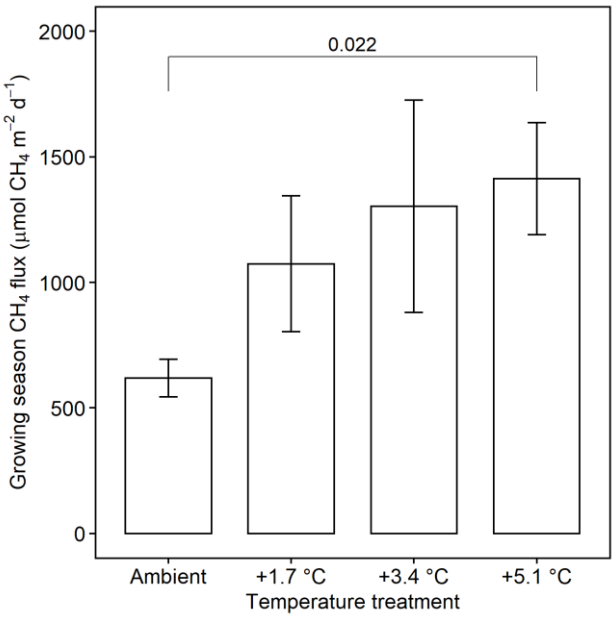


Figure 2. Comparison of $CH_4$ emissions from each warming treatment during the growing season (May-Sep). Means include both the $C_3$ and $C_4$ community and all years of measurement. Error bars indicate SE. Horizonal bars indicate means that are significantly different and the corresponding $p_{adj}$.

229

Mean $CH_4$ emissions were higher from the $C_4$ community than from the $C_3$ community both during the growing season ($F_{1,22}$ = 13.6, $p$ = 0.001; Fig. 3a) and on an annual basis ($F_{1,22}$ = 8.5, $p$ = 0.008; Fig. 3b). Mean annual $CH_4$ emissions ranged from 58 mmol $CH_4$ $m^{-2}$ $yr^{-1}$ (ambient) to 343 mmol $CH_4$ $m^{-2}$ $yr^{-1}$ (+5.1 °C) in the $C_3$ community and from 55 mmol $CH_4$ $m^{-2}$ $yr^{-1}$ (ambient) to 879 mmol $CH_4$ $m^{-2}$ $yr^{-1}$ (+5.1 °C) in the $C_4$ community (Table S2). Under ambient conditions, growing season $CH_4$ fluxes were almost twice as large from $C_4$ plots, whereas under low warming (1.7 to 3.4 °C) this difference increased to more than three times as large (Fig. 3a). From 2017-2019, $CH_4$ emissions were positively related to *Spartina* and

*Distichlis* aboveground biomass across all warming treatments and negatively related to *Schoenoplectus* biomass (Fig. 4a,b). In 2016, however, the direction of those relationships in both plant communities were the exact opposite, with *Spartina* and *Distichlis* biomass negatively related, and *Schoenoplectus* biomass positively related, to $CH_4$ emissions (Fig. 4a,b).

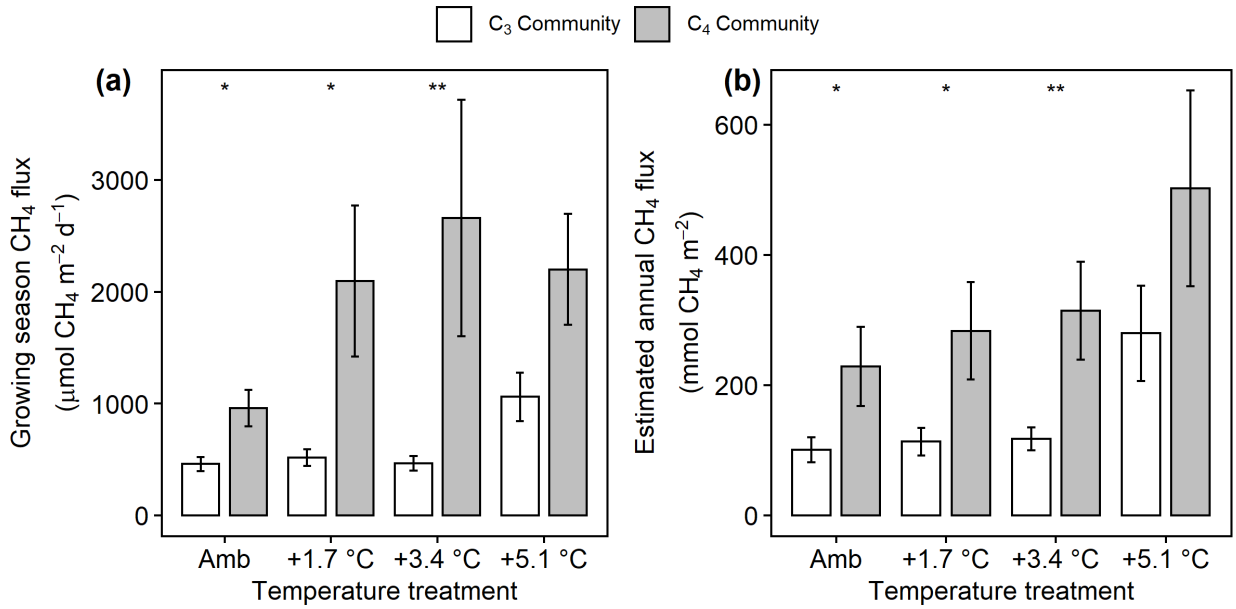


Figure 3. Comparison of $CH_4$ emissions from the $C_3$ community dominated by *Schoenoplectus* (open bars) and the $C_4$ community dominated by *Spartina* and *Distichlis* (grey bars). (a) During the growing season (May-Sep) and (b) scaled to a year. Means are averaged across all sampling dates for 2017 – 2019. Error bars indicate SE. Asterisks indicate significant differences between $C_3$ and $C_4$ means at a given temperature (* $p_{adj}$ <0.05, ** $p_{adj}$ < 0.01).

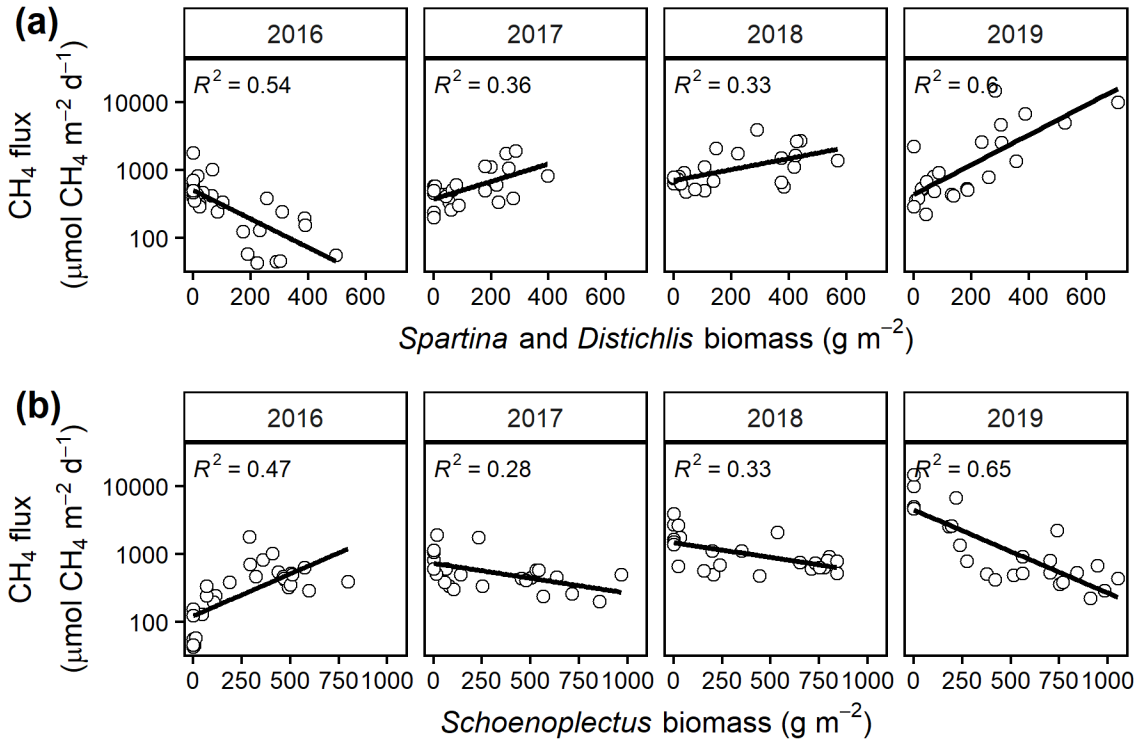


Figure 4. Mean growing season (May-Sep) $CH_4$ emissions from each plot versus the biomass of (a) $C_3$ (*Schoenoplectus*) and (b) $C_4$ (*Spartina* and *Distichlis*) plants. All regressions are significant at $p = 0.05$.

241 3.3 Porewater chemistry

242 Under ambient conditions, porewater collected from the $C_4$ community had more dissolved $CH_4$ ($F_{1,22}$
243 = 18.4, $p < 0.001$; Fig. 5a,b), less $SO_4$ ($F_{1,22}$ = 29.1, $p < 0.001$; Fig 6a), and similar salinity ($p = 0.068$)
244 compared to the $C_3$ community. In the $C_3$ community, warming increased dissolved $CH_4$ in both the
245 rooting zone porewater (10-20 cm) ($F_{3,44}$ = 2.85, $p = 0.048$; Fig. 5a) and in the deep peat (40-120 cm)
246 ($F_{3,44}$ = 6.23, $p = 0.001$; Fig. 5b). Dissolved $CH_4$ concentrations were relatively similar in the ambient,
247 +1.7 °C, and +3.4 °C treatments, but more than doubled with +5.1 °C of warming in both the rooting zone
248 (59 to 125 µmol $CH_4$ $L^{-1}$, $p_{adj}$ <0.001) and the deeper porewater (43 to 1254 µmol $CH_4$ $L^{-1}$, $p_{adj} < 0.001$).
249 In the $C_4$ community there was minimal effect of warming treatment on porewater in the rooting zone
250 ($F_{3,44}$ = 0.442, $p = 0.72$; Fig. 5a), but all levels of warming decreased dissolved $CH_4$ below 40 cm ($F_{3,44}$
251 =129.3, $p < 0.001$), with concentrations in the +3.4 and +5.1 plots less than a third of the concentrations
252 in the ambient plots (155 vs 56 and 40 µmol $CH_4$ $L^{-1}$, $p_{adj} < 0.001$; Fig. 5b).

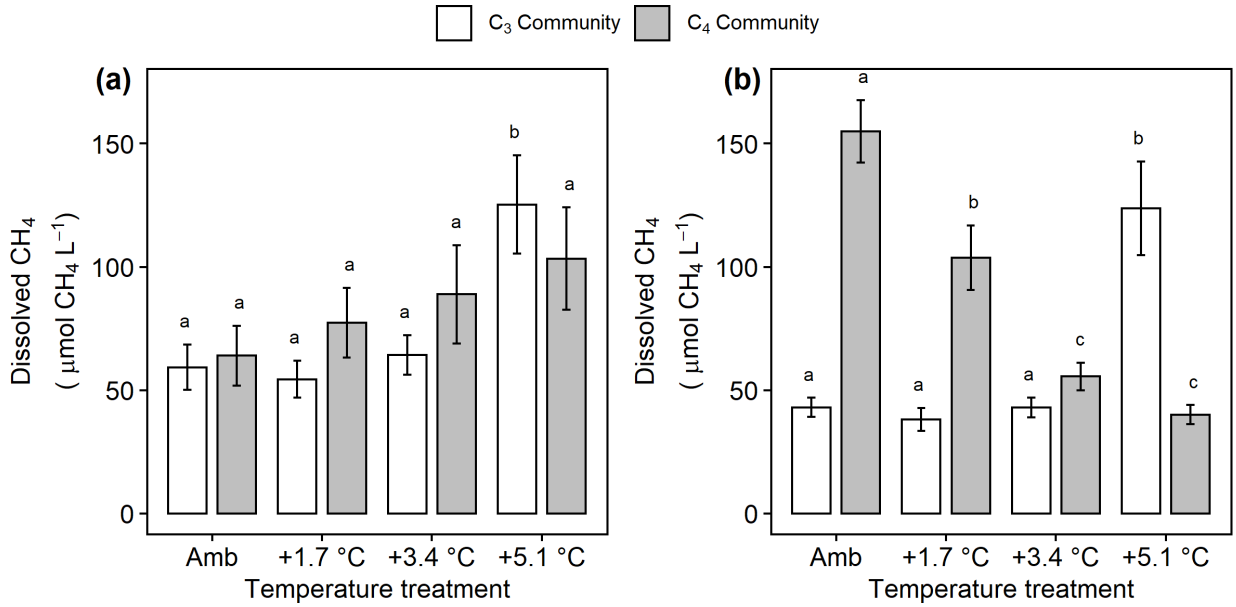


Figure 5. Comparison of dissolved $CH_4$ from the $C_3$ community dominated by *Schoenoplectus* (open bars) and the $C_4$ community dominated by *Spartina* and *Distichlis* (grey bars). (a) In the dominant rooting zone (10-20 cm) and (b) below the rooting zone (40-120 cm). Means are averaged across all sampling dates for 2016 – 2019. Error bars indicate SE. Letters indicate temperature treatments that are significantly different from each other ($p_{adj}$ <0.05) within the same plant community.

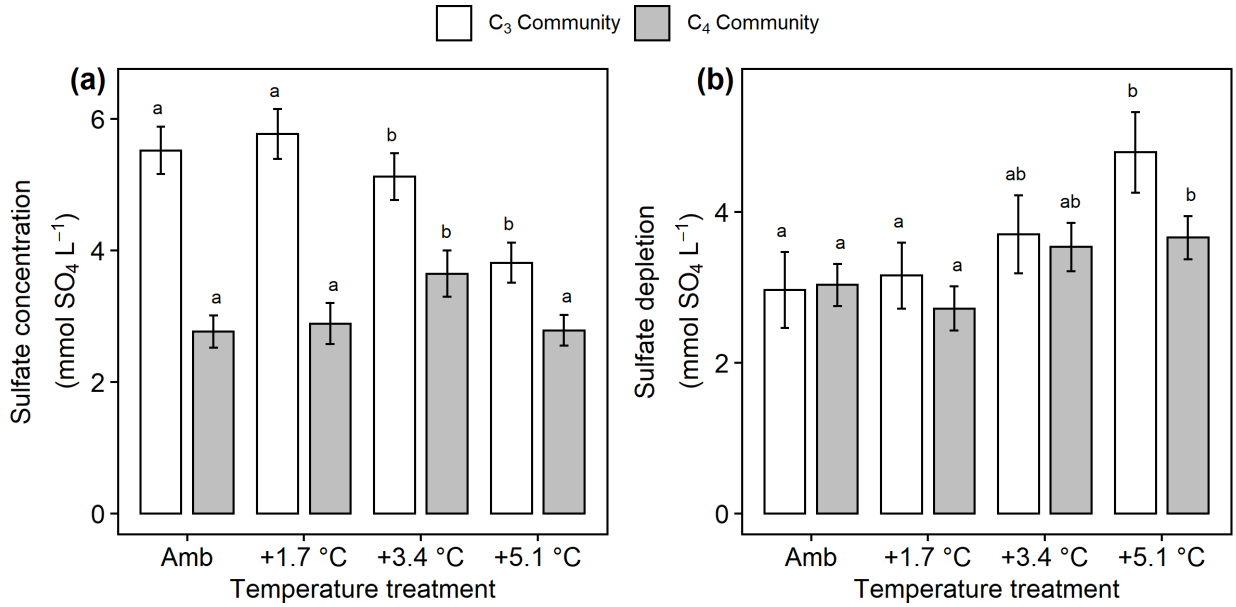


Figure 6. Comparison of sulfate concentrations and estimated sulfate depletion from the $C_3$ community dominated by *Schoenoplectus* (open bars) and the $C_4$ community dominated by *Spartina* and *Distichlis* (grey bars). (a) Sulfate availability throughout the entire soil profile and (b) sulfate depletion in the rooting zone. Means are averaged across all sampling dates for 2016 – 2019. Error bars indicate SE. Letters indicate temperature treatments that are significant different from each other ($p_{adj}$ <0.05) within the same plant community.

In the $C_3$ community, $SO_4$ concentrations decreased with warming ($F_{3,44} = 3.76$, $p = 0.017$), but warming effects on $SO_4$ cycling in the $C_4$ community were more mixed with +3.4 °C increasing $SO_4$ ($p_{adj} = 0.048$) but no other treatments having large effects (Fig. 6a). In all plots, the measured concentrations of rooting-zone $SO_4$ were lower than expected based on salinity (Fig. 6b), indicating that $SO_4$ reduction occurred. In both plant communities, the +5.1 °C treatments increased this $SO_4$-depletion effect compared to ambient, though the effect was stronger in the $C_3$ community ($p < 0.001$) than the $C_4$ community ($p = 0.04$). (Fig. 6b). Dissolved $CH_4$ was highest in both plant communities when $SO_4$ concentrations were < 5 mmol $SO_4$ $L^{-1}$ (Fig. S5).

## 4. Discussion

Soil temperature (both seasonal and experimental) and plant traits were both strong drivers of $CH_4$ emissions from this site. This follows prior field, mesocosm, and incubation studies across a variety of wetlands, in which temperature has been shown to be a strong predictor of $CH_4$ emissions (e.g. Al-Haj and Fulweiler, 2020; van Bodegom and Stams, 1999; Christensen et al., 2003; Dise et al., 1993; Fey and Conrad, 2000; Liu et al., 2019; Ward et al., 2013; Yang et al., 2019; Yvon-Durocher et al., 2014) and in which plant functional type has an interacting effect (e.g. Chen et al., 2017; Duval & Radu, 2018; Liu et al., 2019; Mueller et al., 2020; Ward et al., 2013). Methane emissions are a function of the balance between methanogenesis, $CH_4$ oxidation, and $CH_4$ transport, so explaining these results requires some combination of stimulation of methanogenesis, reduction of $CH_4$ oxidation, or increase in $CH_4$ transport.

Prior data from brackish wetlands are limited, but incubation studies of freshwater wetland soils typically show large increases in $CH_4$ fluxes with warming (Duval & Radu, 2018; Hopple et al., 2020; Inglett et al., 2012; Sihi et al., 2017; van Bodegom & Stams, 1999; Wilson et al., 2016), indicating that warming alters belowground processes. Though there is some evidence that rhizosphere temperature alters $CH_4$ transport through rice aerenchyma (Hosono & Nouchi, 1997), any transport-driven effects in this ecosystem would be transient unless there was a simultaneous increase in net $CH_4$ production (i.e. an increase in methanogenesis that was not completely offset by methanotrophy). Instead, we observed a

sustained increase in $CH_4$ emissions, suggesting large shifts in anaerobic metabolism, especially with +5.1 °C of warming. We propose four potential and non-exclusive mechanisms to explain the temperature-driven increase in $CH_4$ emissions: (1) shifted ratios of $CH_4$ production to oxidation, (2) increased substrate availability, (3) reduced competition with sulfate reducers for $H_2$ and organic C, and (4) indirect plant trait effects (Fig. 7).

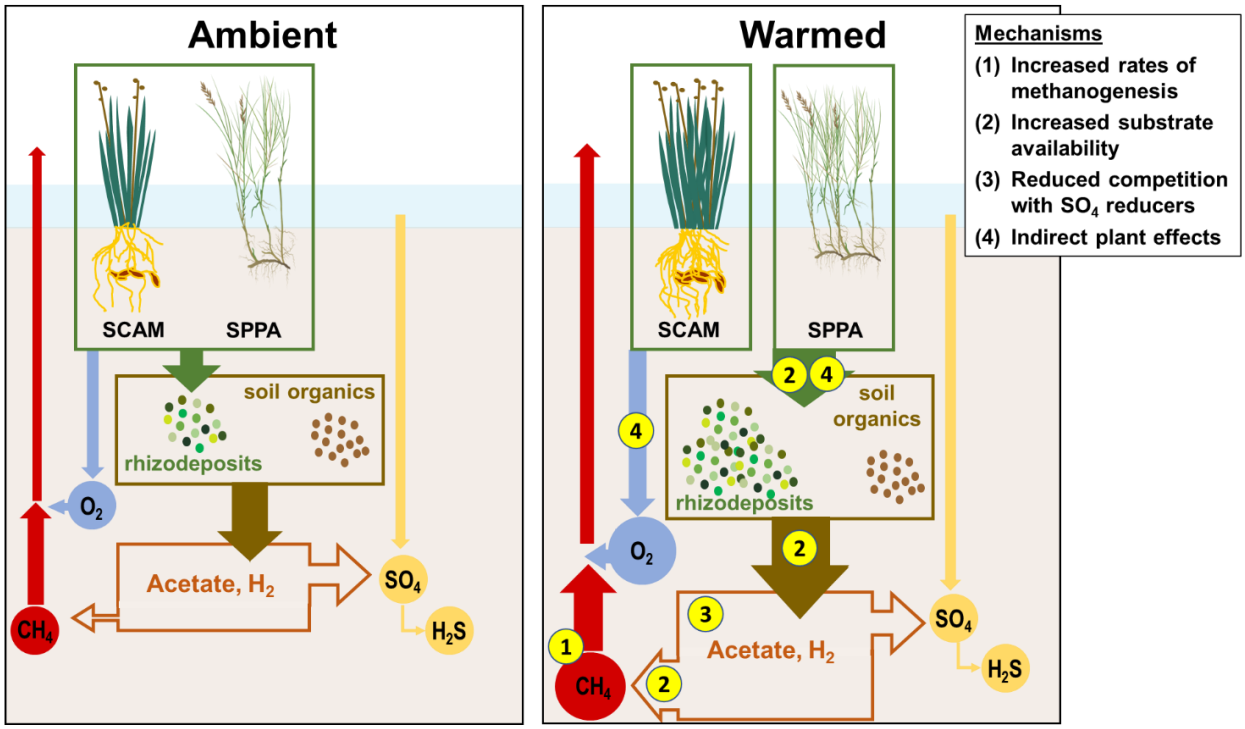


Figure 7. Schematic of mechanisms driving enhanced $CH_4$ emissions in response to warming. SCAM = *Schoenoplectus americanus*. SPPA = *Spartina patens*. Left: Processes under ambient conditions. Plants add organic compounds to the soil, which are transformed into other low-molecular-weight organic compounds. This pool, and processed soil organic matter, support terminal respiration processes dominated by $SO_4$ reduction over $CH_4$ production in organic-rich brackish marsh soils. Plants also transport $O_2$ which supports oxidation of a fraction of the $CH_4$ before it can be transported out of the soil. Right: Processes under warmed conditions. 1) Rates of $CH_4$ production increase more than rates of $CH_4$ oxidation. 2) Substrate availability increases as plants add more rhizodeposits and organic matter is more rapidly fermented to low-molecular-weight organic compounds and $H_2$. 3) The pool of electron donors available to methanogens increases as $SO_4$ reducers become $SO_4$ limited. 4) The dominant plant species have different effects on these process with *S. americanus* driving a net increase in $O_2$ transport and *S. patens* driving a net increase in rhizodeposits.

## 4.1 Whole-ecosystem warming promotes methanogenesis over $CH_4$ oxidation

Holding the supply of substrates and transport properties of the system constant, warming is expected to increase rates of $CH_4$ production relative to $CH_4$ oxidation due solely to differences in the temperature dependence of each process (Megonigal et al., 2016). In wetland soils, the average $Q_{10}$ of methanogenesis

288 is 4.1 compared to 1.9 for aerobic CH4 oxidation (Segers, 1998), which means that a system starting with
289 a given initial ratio between the two processes will become increasingly dominated by methanogenesis as
290 soils warm. A corollary to this expected pattern is that the ratio of the two processes should be constant if
291 the $Q_{10}$ responses are similar, an outcome that was supported with *in situ* measurements of the two
292 processes in a tidal freshwater forested wetland (Megonigal & Schlesinger, 2002). We did not quantify
293 the temperature dependence of $CH_4$ production and oxidation in the present study, but based on the
294 literature (Segers, 1998) it is likely that methanogenic activity increased more than aerobic
295 methanotrophic activity in direct response to warming (Fig. 7, mechanism 1). Evidence for this is that
296 rhizosphere pools of porewater $CH_4$ were highest in the warmest treatment (Fig. 5a); because this
297 occurred despite either no change or an increase in aboveground biomass (Noyce et al., 2019) which
298 would by itself have lowered porewater $CH_4$ due to venting (plant transport), it indicates that $CH_4$
299 production increased relative to the sum of aerobic and anaerobic methane oxidation.

300 4.2 Whole-ecosystem warming increases substrate availability for methanogens

301 Methanogenesis can be the terminal step of anaerobic decomposition, but a consortium of microbes is
302 required to break down soil organic matter to electron donor substrates that methanogens can metabolize.
303 The final step in any decomposition pathway involves the flow of electrons from organic matter (electron
304 donors) to a TEA. Under anaerobic conditions, this is accomplished by microbes that tend to specialize in
305 one TEA and compete for organic C as an electron donor (Megonigal et al., 2004). Consequently, the
306 supply of both electron donors and TEAs regulates the multi-step process of anaerobic decomposition and
307 thus ultimately control $CH_4$ emissions. For all pathways, methanogenic activity is typically limited by the
308 supply of electron donors, including low-molecular-weight organic compounds (e.g. acetate, Neubauer &
309 Craft, 2009) and $H_2$, a product of organic matter fermentation. We propose that whole-ecosystem
310 warming increases the availability of previously limited C substrates in two aspects (Fig. 7, mechanism
311 2).

First, warming may directly influence C availability through biochemical kinetics. Even if organic inputs remained constant, warming likely accelerates fermentation of soil organic matter, increasing substrate availability for methanogens. Second, the warmed plots had longer growing seasons than the unheated controls (Noyce et al., 2019). This presumably increased inputs of root exudates and fresh detritus, accelerating all forms of heterotrophic microbial respiration by providing organic material that is decomposed into low-molecular-weight organic C compounds and $H_2$ (Philippot et al., 2009), stimulating growing season $CH_4$ emissions from warmed plots. In 2017, we observed that gross primary production was positively correlated with $CH_4$ emissions and that this effect increased with warming (Fig. S6). Prior studies have also linked $CH_4$ production or emissions to rates of photosynthesis (Vann & Megonigal, 2003), periods of active growth (Chen et al., 2017; Ward et al., 2013), and plant senescence which coincides with a pulse input of labile C from plants to soils (Bardgett et al., 2005).

Temperature-accelerated biochemical kinetics and increased electron-donor supply are mechanisms that can increase methanogenesis without necessarily shifting methanogenic pathways. However, shifts in the balance between hydrogenotrophic, acetoclastic, and methylotrophic methanogenesis pathways can be expected with warming. For example, in Arctic permafrost, methylotrophic methanogenesis was found to be more sensitive to warming than the other pathways (de Jong et al., 2018). Such shifts can be quantified with future analyses of $H_2$ and low-molecular-weight organic compounds (e.g. Bridgham et al., 2013; Yang et al., 2016), isotopic tracing of specific methanogenic pathways (e.g. Blaser & Conrad, 2016; Conrad, 2005; Neumann et al., 2016; Whiticar, 1999) and molecular community analyses (e.g. Bridgham et al., 2013; He et al., 2015; Wilson et al., 2016).

### 4.4 Whole-ecosystem warming reduces competition with sulfate reducers

While low-molecular-weight organic compounds are electron donors for acetoclastic methanogenic respiration, they are also substrates for other microbial groups such as $SO_4$ reducers (Megonigal et al., 2004; Ye et al., 2014). As a result, consumption of the limited organic carbon supply by $SO_4$ reducers should (and often does) limit methanogenic activity, such that terminal microbial respiration is typically

dominated by $SO_4$ reduction in brackish marshes (Sutton-Grier et al., 2011). Similarly, $SO_4$ reducers are more efficient than methanogens at competing for the $H_2$ required for $CO_2$ reduction (Kristjansson et al., 1982). We did not measure rates of $SO_4$ reduction in this study but can use $SO_4$ depletion as a proxy; more $SO_4$ depletion indicates that more $SO_4$ reduction has occurred. Warming generally increased $SO_4$ depletion, especially in the plots dominated by *Schoenoplectus* (Fig. 6b). Differences in $SO_4$ depletion between plots is not driven by $SO_4$ inputs because the only supply of $SO_4$ is the tidal flow, which is the same for all plots in each community of the experiment. Instead, higher rates of $SO_4$ reduction are most likely driven by some combination of electron donor supply and kinetics. While $SO_4$ reducers likely benefited from the increased availability of electron donors, as described above, the kinetics of $SO_4$ reduction also respond strongly to temperature (Weston & Joye, 2005).

When $SO_4$ concentrations drop below a threshold concentration, $SO_4$ reduction becomes $SO_4$-limited, rather than electron donor-limited (Megonigal et al., 2004). A review of the coastal wetland $CH_4$ literature estimated this threshold at 4 mmol $SO_4$ (Poffenbarger et al., 2011), a value that is consistent with patterns of porewater $CH_4$ and $SO_4$ at the GCReW site (Keller et al. 2009). As $SO_4$ and $O_2$ are the dominant electron-accepting compounds that suppress methanogenesis in this organic soil, this drawdown then releases the methanogens from substrate competition (Fig. 7, mechanism 3). Here, we show that $SO_4$ is typically below 4 mmol in the +5.1 plots in the $C_3$ community and in all plots in the $C_4$ community (Fig. 6, Fig. S5). The drawdown of $SO_4$ may also reduce rates of anaerobic $CH_4$ oxidation (Hinrichs & Boetius, 2003). Van Hulzen et al. (1999) proposed a multi-phase system in a warming incubation experiment, observing that first methanogens are out-competed for substrates by other microbes, next $CH_4$ production increases as the supply of inhibiting TEA decreases, and finally TEA availability is reduced to the point that methanogenesis is controlled only by the supply of electron donors. Warming in this study decreased the time required for the system to pass through the first two phases (van Hulzen et al., 1999). In our experiment, this final phase of increased methanogenic activity occurs when $SO_4$ concentrations dip below 4 mmol $SO_4$ $L^{-1}$, which occurs most often in the +5.1 °C plots, especially in the $C_3$ community. This interpretation is also supported by the long-term record of porewater chemistry from an allied

363 experiment at the site, demonstrating that porewater $CH_4$ concentrations increase as $SO_4$ concentrations
364 decrease (Keller et al., 2009).
365 Methanogens may also have a competitive advantage over $SO_4$ reducers for electron donor
366 consumption at warmer temperatures (van Hulzen et al., 1999). Sulfate reducers and methanogens have
367 very similar $K_M$ values for acetate, but the $K_M$ for acetoclastic methanogenesis may decrease with
368 temperature whereas $K_M$ values for $SO_4$ reducers increase with temperature (van Bodegom & Stams,
369 1999). If this is the case in our system then warming would allow methanogens to use a greater proportion
370 of the available substrates.
371 4.5 Plant traits modify warming effects on $CH_4$ cycling
372 The three biogeochemical mechanisms we propose to explain a warming-induced increase in $CH_4$
373 emissions should interact strongly with plant responses to warming. Relationships between plant
374 functional groups and $CH_4$ emissions have been demonstrated through field studies in other wetland
375 ecosystems such as peatlands (Bubier et al., 1995; Ward et al., 2013) and in tidal wetland mesocosms (Liu
376 et al., 2019; Martin & Moseman-Valtierra, 2017; Mueller et al., 2020). We provide field evidence that
377 two species with distinct plant traits -- *Schoenoplectus* and *Spartina* -- have strikingly different effects on
378 $CH_4$ emissions from brackish wetlands. *Spartina*-dominated communities had consistently higher $CH_4$
379 emissions under both ambient and warmed conditions (Fig. 3). In most years, *Schoenoplectus* biomass
380 was negatively correlated with $CH_4$ emissions, while *Spartina*/*Distichlis* biomass was positively
381 correlated. Vegetation effects are typically strongest during the growing season, when the plants are
382 actively altering rhizosphere biogeochemistry (van der Nat & Middelburg, 1998; Ward et al., 2013),
383 which is consistent with our observations in this study.
384 As with warming effects, plant-driven shifts in $CH_4$ emissions are the result of differing rates of $CH_4$
385 production, oxidation, transport, or a combination of these processes, but sustained differences in
386 emissions cannot be attributed only to transport, as discussed previously. Instead, the stimulation of $CH_4$
387 emissions is likely due to changes in the plant-mediated supply of electron acceptors and electron donors.

In a field environment, differentiating between species-specific effects and underlying environmental conditions can be difficult, but mesocosm studies that control all environmental factors have also found species-specific effects on $CH_4$ cycling (e.g. Liu et al., 2014). Plants can alter $CH_4$ cycling by adding $O_2$ (electron acceptor) or C substrates (electron donors) to the rhizosphere, altering the redox state. We propose that *Schoenoplectus* is a net oxidizer of the rhizosphere and that *Spartina* is a net reducer, and thus their presence and productivity have opposing effects on $CH_4$ emissions (Fig. 7, mechanism 4).

*4.5.1 Schoenoplectus oxidizes the rhizosphere, increasing $CH_4$ oxidation*

Species vary in their capacity to support aerobic $CH_4$ oxidation (van der Nat & Middelburg, 1998) and *Schoenoplectus* appears to support higher rates of aerobic $CH_4$ oxidation than *Spartina* (Mueller et al., 2020). *Scirpus lacustris* is morphologically similar to *Schoenoplectus americanus* studied here and has been demonstrated to have substantial rhizosphere oxidation capacity, especially during the growing season (van der Nat & Middelburg, 1998). Consequently, these plants likely exert stronger control on rates of $CH_4$ oxidation than rates of methanogenesis (van der Nat & Middelburg, 1998). We hypothesize that the relatively high capacity of *Schoenoplectus* to transport $O_2$ held the $CH_4$ emissions stimulation caused by modest levels of warming (+1.7 to +3.4 °C) to rates similar to under ambient conditions (Fig. 3). At high warming (+5.1 °C), however, *Schoenoplectus* community $CH_4$ emissions drastically increase (Fig. 3). We suggest that this is due to the combined effects of the three mechanisms discussed previously, namely the differences in the $Q_{10}$-values of $CH_4$ production and $CH_4$ oxidation, the increased supply of organic substrate through plant productivity, and the decrease in competition for electron donors due to $SO_4$ depletion. Collectively, when the ecosystem is warmed above current ambient conditions by 5 °C or more, enhanced stimulation of $CH_4$ production starts to offset some of the *Schoenoplectus* oxidation effect. This also offers an explanation for the positive correlation between *Schoenoplectus* biomass and $CH_4$ emissions observed in 2016 as that was the hottest of the four years in this study.

*4.5.2 Spartina reduces the rhizosphere, increasing $CH_4$ production*

The variability in quality and quantity of root exudates between plant functional types is well known to affect microbial community composition and activity (Deyn et al., 2008). Methanogenesis responses to warming in incubation studies are related to the lignin and cellulose content of the peat, which in turn depends on the plant functional type from which the peat developed (Duval & Radu, 2018). Although warming is likely increasing substrate availability across the whole experiment, the production of labile, low-molecular-weight C substrates through fermentation is less sensitive to temperature above 25 °C than below this threshold (Neubauer & Craft, 2009; Weston & Joye, 2005). Microorganisms may also preferentially use freshly produced (i.e. labile) organic carbon compounds as electron donors (DeLaune et al., 2014) and consequently warming effects on $CH_4$ production should be strongest in a system where rates of root exudation and turnover are most rapid. We propose that root exudation and turnover explain the positive correlation between plan t biomass and $CH_4$ emissions that we observed in the $C_4$ community. Multiple years of porewater chemistry at this site show that *Spartina*-dominated communities have higher DOC and dissolved $CH_4$ than adjacent *Schoenoplectus* communities (Keller et al., 2009; Marsh et al., 2005). Though we did not directly measure root exudation, porewater DOC is partially derived from root exudates and has been used as a proxy to understand the responses of root exudates to global change factors (Dieleman et al., 2016; Fenner et al., 2007; Jones et al., 2009).

We observed a simultaneous increase in dissolved $CH_4$ at the soil surface and a decrease in dissolved $CH_4$ at depth in the warmed $C_4$ plots. As with the observed trends in $CH_4$ emissions, there are multiple mechanisms that could cause a shift in porewater $CH_4$ concentrations. Of the four mechanisms outlined above, perhaps the simplest explanation is an increase in labile C at shallow depths and a decrease in deeper soil. This is consistent with DOC depth profiles from this the $C_4$ community in which porewater DOC increases with warming in shallow samples but decreases with warming in deep samples (Fig. S7). This shallowing of peak DOC concentrations could be due to a warming-induced increase in evapotranspiration, leading to slower downward hydrologic transport of DOC-rich surface porewater to

lower depths, or a warming-induced shallowing of the root system, leading to a shift in the location of root exudates.

In most years, *Spartina* biomass was positively correlated with $CH_4$ emissions, supporting our hypothesis that *Spartina* favors net $CH_4$ production. However, in 2016 *Spartina* biomass and $CH_4$ emissions were negatively correlated. Prior work at this site has indicated that *Spartina*/*Distichlis* biomass is more negatively affected by hot and dry growing conditions than *Schoenoplectus* (Noyce et al., 2019) due in part because the *Spartina*/*Distichlis* ($C_4$) communities are less frequently inundated. The 2016 growing season was substantially warmer than average (Table 2) and the heating treatments were initialized on 1 Jun of that year, after the annual plants had already established and may have developed adaptations to ambient, rather than elevated, temperature conditions. The combination of these two effects likely led to heat stress, reducing the root exudates supplied to the rhizosphere microbial community (Heckathorn et al., 2013) and thus minimizing the *Spartina* stimulation effect.

4.6 Comparisons with prior data

Methane emissions have been measured at the GCReW site previously, but this study represents the most comprehensive dataset collected to date, and is thus particularly useful for advancing the process-based understanding needed to improve prognostic models. Overall, our flux estimates are lower than those reported previously. The earliest $CH_4$ fluxes were measured in a single month (July) in *Schoenoplectus*-dominated plots and reported to be 331 to 6883 μmol $m^{-2}$ $d^{-1}$ (Dacey et al., 1994), much higher than our range of 359 to 1651 μmol $m^{-2}$ $d^{-1}$ for ambient temperature *Schoenoplectus* plots in July. Similarly, Marsh et al. (2005) reported mean growing season (May-Oct) $CH_4$ emissions from this site of 846 ± 111 μmol $CH_4$ $m^{-2}$ $d^{-1}$, whereas we measured 656 ± 79 μmol $CH_4$ $m^{-2}$ $d^{-1}$ over the same months. Finally, Pastore et al. (2017) estimated average annual fluxes in their *Schoenoplectus*-dominated ambient $CO_2$ plots as 3.1 ± 1.7 g $CH_4$ $m^{-2}$ $yr^{-1}$, compared to our estimates of 1.6 ± 0.3 g $CH_4$ $m^{-2}$ $yr^{-1}$ for *Schoenoplectus* plots. The different estimates by these studies may be partly due to interannual variability as demonstrated in our data where 2018 had substantially higher fluxes than any of the surrounding years (Table S2).

462 The annual estimates reported here for ambient temperature plots trended lower than published
463 mean $CH_4$ emissions for mesohaline tidal marshes. Our plots ranged from 0.7 to 9.3 g $CH_4$ $m^{-2}$ $yr^{-1}$ (mean
464 = 9.3), compared to the range of 3.3 to 16.4 g $CH_4$ $m^{-2}$ $yr^{-1}$ (mean = 16.4) reported by Poffenbarger et al.
465 (2011). This difference may be explained by the fact that there was significant within-class variation in
466 the oligohaline and mesohaline salinity classes that was unexplained and their assessment was based on
467 too few data points to fully capture the variation that is expected to exist in the mesohaline class. Indeed,
468 subsequent studies have documented fluxes well below 3 g $CH_4$ $m^{-2}$ $yr^{-1}$ (Krauss & Whitbeck, 2012), and
469 even negative fluxes (Al-Haj & Fulweiler, 2020). We hypothesize that the low fluxes measured at our site
470 reflect *Schoenoplectus americanus* traits that favor $CH_4$ oxidation more than $CH_4$ production, and that the
471 high end of our range was limited by the high soil elevation (i.e. deep water table) of areas dominated by
472 *Spartina patens*, off-setting the influence of *S. patens* traits that favor $CH_4$ production.

473 4.7 Implications for tidal wetland carbon cycling

474 Warming accelerates rates of $CH_4$ emissions from brackish marshes, especially during the growing
475 season. This is driven by both direct and indirect warming effects and mediated by soil biogeochemistry,
476 but the magnitude of the warming effect is also dependent on traits of the plant species that dominate the
477 plant community. Communities dominated by *Spartina patens* increase net $CH_4$ emissions in response to
478 smaller increments of warming than communities dominated by *Schoenoplectus americanus*. *Spartina*-
479 dominated sites may thus have a higher likelihood of shifting from a net C sink to a net C source under
480 future warming conditions, due to this increased loss of C as $CH_4$. However, this effect could be mitigated
481 if these high-elevation *Spartina* marshes become dominated by *Schoenoplectus* in response to predicted
482 accelerated sea-level rise (Kirwan & Guntenspergen, 2012). In addition, *Spartina* traits are plastic and
483 influenced by factors such as soil redox conditions (Kludze & DeLaune, 1994), salinity (Crozier &
484 DeLaune, 1996), and water level (Liu et al., 2019), all of which can be expected to change plant-mediated
485 effects on $CH_4$ biogeochemistry. Further studies are needed to thoroughly assess the range of

environmental conditions under which *Spartina* is a net reducer and *Schoenoplectus* is a net oxidizer as proposed by the present study.

## Data availability

All data is available from the corresponding author upon request.

## Author contributions

GLN and JPM designed the study, GLN collected and analyzed the data, and GLN and JPM wrote the paper.

## Competing interests

The authors declare that they have no conflict of interest.

## Acknowledgements

This manuscript is based upon work supported by the U.S. Department of Energy, Office of Science, Office of Biological and Environmental Research Program (DE-SC0014413 and DE-SC0019110), the National Science Foundation Long-Term Research in Environmental Biology Program (DEB-0950080, DEB-1457100, and DEB-1557009), and the Smithsonian Institution. Roy Rich designed the warming infrastructure and maintains it with the assistance of Gary Peresta. We also thank technicians in the SERC Biogeochemistry Lab for assistance with porewater collection and analysis.

## References

Al-Haj, A. N., & Fulweiler, R. W. (2020). A synthesis of methane emissions from shallow vegetated coastal ecosystems. *Global Change Biology*, *26*(5), 2988–3005. https://doi.org/10.1111/gcb.15046

510 Bardgett, R. D., Bowman, W. D., Kaufmann, R., & Schmidt, S. K. (2005). A temporal approach to
511 linking aboveground and belowground ecology. *Trends in Ecology & Evolution*, *20*(11), 634–641.
512 https://doi.org/10.1016/j.tree.2005.08.005
513 Basiliko, N., Stewart, H., Roulet, N. T., & Moore, T. R. (2012). Do root exudates enhance peat
514 decomposition? *Geomicrobiology Journal*, *29*(4), 374–378.
515 https://doi.org/10.1080/01490451.2011.568272
516 Bianchi, T. S. (2006). *Biogeochemistry of Estuaries*. Oxford University Press.
517 Blaser, M., & Conrad, R. (2016). Stable carbon isotope fractionation as tracer of carbon cycling in anoxic
518 soil ecosystems. *Current Opinion in Biotechnology*, *41*, 122–129.
519 https://doi.org/10.1016/j.copbio.2016.07.001
520 Bridgham, S. D., Cadillo-Quiroz, H., Keller, J. K., & Zhuang, Q. (2013). Methane emissions from
521 wetlands: Biogeochemical, microbial, and modeling perspectives from local to global scales. *Global*
522 *Change Biology*, *19*(5), 1325–1346. https://doi.org/10.1111/gcb.12131
523 Bridgham, S. D., Megonigal, J. P., Keller, J. K., Bliss, N. B., & Trettin, C. (2006). The carbon balance of
524 North American wetlands. *Wetlands*, *26*(4), 889–916. https://doi.org/10.1672/0277-
525 5212(2006)26[889:TCBONA]2.0.CO;2
526 Bubier, J. L., Moore, T. R., Bellisario, L., Comer, N. T., & Crill, P. M. (1995). Ecological controls on
527 methane emissions from a Northern Peatland Complex in the zone of discontinuous permafrost,
528 Manitoba, Canada. *Global Biogeochemical Cycles*, *9*(4), 455–470.
529 https://doi.org/10.1029/95GB02379
530 Chen, J., Luo, Y., Xia, J., Wilcox, K. R., Cao, J., Zhou, X., Jiang, L., Niu, S., Estera, K. Y., Huang, R.,
531 Wu, F., Hu, T., Liang, J., Shi, Z., Guo, J., & Wang, R.-W. (2017). Warming effects on ecosystem
532 carbon fluxes are modulated by plant functional types. *Ecosystems*, *20*(3), 515–526.
533 https://doi.org/10.1007/s10021-016-0035-6
534 Christensen, T. R., Ekberg, A., Ström, L., Mastepanov, M., Panikov, N., Öquist, M., Svensson, B. H.,
535 Nykänen, H., Martikainen, P. J., & Oskarsson, H. (2003). Factors controlling large scale variations in

methane emissions from wetlands. *Geophysical Research Letters*, *30*(7), 1414. https://doi.org/10.1029/2002GL016848

Conrad, R. (2005). Quantification of methanogenic pathways using stable carbon isotopic signatures: A review and a proposal. *Organic Geochemistry*, *36*(5), 739–752. https://doi.org/10.1016/j.orggeochem.2004.09.006

Conrad, R. (2020). Importance of hydrogenotrophic, aceticlastic and methylotrophic methanogenesis for methane production in terrestrial, aquatic and other anoxic environments: A mini review. *Pedosphere*, *30*(1), 25–39. https://doi.org/10.1016/S1002-0160(18)60052-9

Crozier, C. R., & DeLaune, R. D. (1996). Methane production by soils from different Louisiana marsh vegetation types. *Wetlands*, *16*(2), 121–126. https://doi.org/10.1007/BF03160685

Dacey, J. W. H., Drake, B. G., & Klug, M. J. (1994). Stimulation of methane emission by carbon dioxide enrichment of marsh vegetation. *Nature*, *370*(6484), 47–49. https://doi.org/10.1038/370047a0

de Jong, A. E. E., in 't Zandt, M. H., Meisel, O. H., Jetten, M. S. M., Dean, J. F., Rasigraf, O., & Welte, C. U. (2018). Increases in temperature and nutrient availability positively affect methane-cycling microorganisms in Arctic thermokarst lake sediments. *Environmental Microbiology*, *20*(12), 4314–4327. https://doi.org/10.1111/1462-2920.14345

Delarue, F., Gogo, S., Buttler, A., Bragazza, L., Jassey, V. E. J., Bernard, G., & Laggoun-Défarge, F. (2014). Indirect effects of experimental warming on dissolved organic carbon content in subsurface peat. *Journal of Soils and Sediments*, *14*(11), 1800–1805. https://doi.org/10.1007/s11368-014-0945-x

Deyn, G. B. D., Cornelissen, J. H. C., & Bardgett, R. D. (2008). Plant functional traits and soil carbon sequestration in contrasting biomes. *Ecology Letters*, *11*(5), 516–531. https://doi.org/10.1111/j.1461-0248.2008.01164.x

Dieleman, C. M., Lindo, Z., McLaughlin, J. W., Craig, A. E., & Branfireun, B. A. (2016). Climate change effects on peatland decomposition and porewater dissolved organic carbon biogeochemistry. *Biogeochemistry*, *128*(3), 385–396. https://doi.org/10.1007/s10533-016-0214-8

561 Ding, W., Cai, Z., & Tsuruta, H. (2005). Plant species effects on methane emissions from freshwater
562 marshes. *Atmospheric Environment*, *39*(18), 3199–3207.
563 https://doi.org/10.1016/j.atmosenv.2005.02.022
564 Dise, N. B., Gorham, E., & Verry, E. S. (1993). Environmental factors controlling methane emissions
565 from peatlands in northern Minnesota. *Journal of Geophysical Research: Atmospheres*, *98*(D6),
566 10583–10594. https://doi.org/10.1029/93JD00160
567 Duval, T. P., & Radu, D. D. (2018). Effect of temperature and soil organic matter quality on greenhouse-
568 gas production from temperate poor and rich fen soils. *Ecological Engineering*, *114*, 66–75.
569 https://doi.org/10.1016/j.ecoleng.2017.05.011
570 Environmental Protection Agency. (2017). *Inventory of U.S. Greenhouse Gas Emissions and Sinks: 1990-*
571 *2015*. (EPA 430-P-17-001).
572 Fenner, N., Freeman, C., Lock, M. A., Harmens, H., Reynolds, B., & Sparks, T. (2007). Interactions
573 between elevated $CO_2$ and warming could amplify DOC exports from peatland catchments.
574 *Environmental Science & Technology*, *41*(9), 3146–3152. https://doi.org/10.1021/es061765v
575 Fey, A., & Conrad, R. (2000). Effect of temperature on carbon and electron flow and on the archaeal
576 community in methanogenic rice field soil. *Applied and Environmental Microbiology*, *66*(11), 4790–
577 4797. https://doi.org/10.1128/AEM.66.11.4790-4797.2000
578 He, S., Malfatti, S. A., McFarland, J. W., Anderson, F. E., Pati, A., Huntemann, M., Tremblay, J., Rio, T.
579 G. del, Waldrop, M. P., Windham-Myers, L., & Tringe, S. G. (2015). Patterns in wetland microbial
580 community composition and functional gene repertoire associated with methane emissions. *MBio*,
581 *6*(3), e00066-15. https://doi.org/10.1128/mBio.00066-15
582 Heckathorn, S. A., Giri, A., Mishra, S., & Bista, D. (2013). Heat Stress and Roots. In *Climate Change*
583 *and Plant Abiotic Stress Tolerance* (pp. 109–136). John Wiley & Sons, Ltd.
584 https://doi.org/10.1002/9783527675265.ch05
585 Hinrichs, K.-U., & Boetius, A. (2003). The Anaerobic Oxidation of Methane: New Insights in Microbial
586 Ecology and Biogeochemistry. In G. Wefer, D. Billett, D. Hebbeln, B. B. Jørgensen, M. Schlüter, &

T. C. E. van Weering (Eds.), *Ocean Margin Systems* (pp. 457–477). Springer. https://doi.org/10.1007/978-3-662-05127-6_28

Holmquist, J. R., Windham-Myers, L., Bliss, N., Crooks, S., Morris, J. T., Megonigal, J. P., Troxler, T., Weller, D., Callaway, J., Drexler, J., Ferner, M. C., Gonneea, M. E., Kroeger, K. D., Schile-Beers, L., Woo, I., Buffington, K., Breithaupt, J., Boyd, B. M., Brown, L. N., … Woodrey, M. (2018). Accuracy and precision of tidal wetland soil carbon mapping in the conterminous United States. *Scientific Reports*, *8*(1), 9478. https://doi.org/10.1038/s41598-018-26948-7

Hopple, A. M., Wilson, R. M., Kolton, M., Zalman, C. A., Chanton, J. P., Kostka, J., Hanson, P. J., Keller, J. K., & Bridgham, S. D. (2020). Massive peatland carbon banks vulnerable to rising temperatures. *Nature Communications*, *11*(1), 2373. https://doi.org/10.1038/s41467-020-16311-8

Hosono, T., & Nouchi, I. (1997). The dependence of methane transport in rice plants on the root zone temperature. *Plant and Soil*, *191*(2), 233–240. https://doi.org/10.1023/A:1004203208686

Inglett, K. S., Inglett, P. W., Reddy, K. R., & Osborne, T. Z. (2012). Temperature sensitivity of greenhouse gas production in wetland soils of different vegetation. *Biogeochemistry*, *108*(1–3), 77–90. https://doi.org/10.1007/s10533-011-9573-3

IPCC. (2013). *Limate Change 2013: The Physical Science Basis. Working Group I Contribution to the Fifth Assessment Report of the Intergovernmental Panel on Climate Change*. www.ipcc.ch/report/ar5/wg1/

Jones, T. G., Freeman, C., Lloyd, A., & Mills, G. (2009). Impacts of elevated atmospheric ozone on peatland below-ground DOC characteristics. *Ecological Engineering*, *35*(6), 971–977. https://doi.org/10.1016/j.ecoleng.2008.08.009

Kayranli, B., Scholz, M., Mustafa, A., & Hedmark, Å. (2010). Carbon storage and fluxes within freshwater wetlands: A critical review. *Wetlands*, *30*(1), 111–124. https://doi.org/10.1007/s13157-009-0003-4

Keller, J. K., Wolf, A. A., Weisenhorn, P. B., Drake, B. G., & Megonigal, J. P. (2009). Elevated $CO_2$ affects porewater chemistry in a brackish marsh. *Biogeochemistry*, *96*(1–3), 101–117. https://doi.org/10.1007/s10533-009-9347-3

Kirwan, M. L., & Guntenspergen, G. R. (2012). Feedbacks between inundation, root production, and shoot growth in a rapidly submerging brackish marsh. *Journal of Ecology*, *100*(3), 764–770. https://doi.org/10.1111/j.1365-2745.2012.01957.x

Kludze, H. K., & DeLaune, R. D. (1994). Methane emissions and growth of *Spartina patens* in response to soil redox intensity. *Soil Science Society of America Journal*, *58*(6), 1838–1845. https://doi.org/10.2136/sssaj1994.03615995005800060037x

Krauss, K. W., & Whitbeck, J. L. (2012). Soil greenhouse gas fluxes during wetland forest retreat along the Lower Savannah River, Georgia (USA). In *Wetlands* (Vol. 32, Issue 1, p. 7381). https://doi.org/10.1007/s13157-011-0246-8

Kristjansson, J. K., Schönheit, P., & Thauer, R. K. (1982). Different Ks values for hydrogen of methanogenic bacteria and sulfate reducing bacteria: An explanation for the apparent inhibition of methanogenesis by sulfate. *Archives of Microbiology*, *131*(3), 278–282. https://doi.org/10.1007/BF00405893

Lenzewski, N., Mueller, P., Meier, R. J., Liebsch, G., Jensen, K., & Koop-Jakobsen, K. (2018). Dynamics of oxygen and carbon dioxide in rhizospheres of Lobelia dortmanna – a planar optode study of belowground gas exchange between plants and sediment. *New Phytologist*, n/a-n/a. https://doi.org/10.1111/nph.14973

Liu, D., Ding, W., Yuan, J., Xiang, J., & Lin, Y. (2014). Substrate and/or substrate-driven changes in the abundance of methanogenic archaea cause seasonal variation of methane production potential in species-specific freshwater wetlands. *Applied Microbiology and Biotechnology*, *98*(10), 4711–4721. https://doi.org/10.1007/s00253-014-5571-4

635 Liu, L., Wang, D., Chen, S., Yu, Z., Xu, Y., Li, Y., Ge, Z., & Chen, Z. (2019). Methane emissions from
636 estuarine coastal wetlands: Implications for global change effect. *Soil Science Society of America*
637 *Journal*, *83*(5), 1368–1377. https://doi.org/10.2136/sssaj2018.12.0472
638 Lu, M., Caplan, J. S., Bakker, J. D., Langley, J. A., Mozdzer, T. J., Drake, B. G., & Megonigal, J. P.
639 (2016). Allometry data and equations for coastal marsh plants. *Ecology*, *97*(12), 3554–3554.
640 https://doi.org/10.1002/ecy.1600
641 Marsh, A. S., Rasse, D. P., Drake, B. G., & Patrick Megonigal, J. (2005). Effect of elevated $CO_2$ on
642 carbon pools and fluxes in a brackish marsh. *Estuaries*, *28*(5), 694–704.
643 https://doi.org/10.1007/BF02732908
644 Martin, R. M., & Moseman-Valtierra, S. (2017). Different short-term responses of greenhouse gas fluxes
645 from salt marsh mesocosms to simulated global change drivers. *Hydrobiologia*, *802*(1), 71–83.
646 https://doi.org/10.1007/s10750-017-3240-1
647 Mcleod, E., Chmura, G. L., Bouillon, S., Salm, R., Björk, M., Duarte, C. M., Lovelock, C. E.,
648 Schlesinger, W. H., & Silliman, B. R. (2011). A blueprint for blue carbon: Toward an improved
649 understanding of the role of vegetated coastal habitats in sequestering $CO_2$. *Frontiers in Ecology and*
650 *the Environment*, *9*(10), 552–560. https://doi.org/10.1890/110004
651 Megonigal, J. P., Whalen, S. C., Tissue, D. T., Bovard, B. D., Allen, A. S., & Albert, D. B. (1999). A
652 plant-soil-atmosphere microcosm for tracing radiocarbon from photosynthesis through
653 methanogenesis. *Soil Science Society of America Journal*, *63*(3), 665–671.
654 https://doi.org/10.2136/sssaj1999.03615995006300030033x
655 Megonigal, J. Patrick, Hines, M. E., & Visscher, P. T. (2004). Anaerobic metabolism: Linkages to trace
656 gases and aerobic processes. In W. H. Schlesinger (Ed.), *Biogeochemistry* (pp. 317–424). Elsevier-
657 Pergamon.
658 Megonigal, J. Patrick, & Schlesinger, William. H. (2002). Methane-limited methanotrophy in tidal
659 freshwater swamps. *Global Biogeochemical Cycles*, *16*(4), 1088.
660 https://doi.org/10.1029/2001GB001594

Moor, H., Rydin, H., Hylander, K., Nilsson, M. B., Lindborg, R., & Norberg, J. (2017). Towards a trait-based ecology of wetland vegetation. *Journal of Ecology*, *105*(6), 1623–1635. https://doi.org/10.1111/1365-2745.12734

Mueller, P., Jensen, K., & Megonigal, J. P. (2016). Plants mediate soil organic matter decomposition in response to sea level rise. *Global Change Biology*, *22*(1), 404–414. https://doi.org/10.1111/gcb.13082

Mueller, P., Mozdzer, T. J., Langley, J. A., Aoki, L. R., Noyce, G. L., & Megonigal, J. P. (2020). Plants determine methane response to sea level rise. *Nature Communications*. https://doi.org/10.1038/s41467-020-18763-4

Neubauer, S. C., Emerson, D., & Megonigal, J. P. (2008). Microbial oxidation and reduction of Iron in the root zone and influences on metal mobility. In *Biophysico-Chemical Processes of Heavy Metals and Metalloids in Soil Environments* (pp. 339–371). John Wiley & Sons, Ltd. https://doi.org/10.1002/9780470175484.ch9

Neubauer, Scott C, & Craft, C. B. (2009). Chapter 23 Global Change and Tidal Freshwater Wetlands: Scenarios and Impacts. In A. Barendregt, D. Whigham, & A. Baldwin (Eds.), *Tidal Freshwater Wetlands* (pp. 253–310). Margraf Publishers.

Neubauer, Scott C., & Megonigal, J. P. (2015). Moving beyond global warming potentials to quantify the climatic role of ecosystems. *Ecosystems*, *18*(6), 1000–1013. https://doi.org/10.1007/s10021-015-9879-4

Neumann, R. B., Blazewicz, S. J., Conaway, C. H., Turetsky, M. R., & Waldrop, M. P. (2016). Modeling $CH_4$ and $CO_2$ cycling using porewater stable isotopes in a thermokarst bog in Interior Alaska: Results from three conceptual reaction networks. *Biogeochemistry*, *127*(1), 57–87. https://doi.org/10.1007/s10533-015-0168-2

Noyce, G. L., Kirwan, M. L., Rich, R. L., & Megonigal, J. P. (2019). Asynchronous nitrogen supply and demand produce non-linear plant allocation responses to warming and elevated $CO_2$. *Proceedings of the National Academy of Sciences*.

686 Oremland, R. S., Marsh, L. M., & Polcin, S. (1982). Methane production and simultaneous sulphate
687 reduction in anoxic, salt marsh sediments. *Nature*, *296*(5853), 143–145.
688 https://doi.org/10.1038/296143a0
689 Pastore, M. A., Megonigal, J. P., & Langley, J. A. (2017). Elevated $CO_2$ and nitrogen addition accelerate
690 net carbon gain in a brackish marsh. *Biogeochemistry*, *133*(1), 73–87. https://doi.org/10.1007/s10533-
691 017-0312-2
692 Pendleton, L., Donato, D. C., Murray, B. C., Crooks, S., Jenkins, W. A., Sifleet, S., Craft, C., Fourqurean,
693 J. W., Kauffman, J. B., Marbà, N., Megonigal, P., Pidgeon, E., Herr, D., Gordon, D., & Baldera, A.
694 (2012). Estimating global "blue carbon" emissions from conversion and degradation of vegetated
695 coastal ecosystems. *PLOS ONE*, *7*(9), e43542. https://doi.org/10.1371/journal.pone.0043542
696 Philippot, L., Hallin, S., Börjesson, G., & Baggs, E. M. (2009). Biochemical cycling in the rhizosphere
697 having an impact on global change. *Plant and Soil*, *321*(1), 61–81. https://doi.org/10.1007/s11104-
698 008-9796-9
699 Poffenbarger, H. J., Needelman, B. A., & Megonigal, J. P. (2011). Salinity influence on methane
700 emissions from tidal marshes. *Wetlands*, *31*(5), 831–842. https://doi.org/10.1007/s13157-011-0197-0
701 Rich, R. L., Stefanski, A., Montgomery, R. A., Hobbie, S. E., Kimball, B. A., & Reich, P. B. (2015).
702 Design and performance of combined infrared canopy and belowground warming in the B4WarmED
703 (Boreal Forest Warming at an Ecotone in Danger) experiment. *Global Change Biology*, *21*(6), 2334–
704 2348. https://doi.org/10.1111/gcb.12855
705 Robroek, B. J. M., Albrecht, R. J. H., Hamard, S., Pulgarin, A., Bragazza, L., Buttler, A., & Jassey, V. E.
706 (2016). Peatland vascular plant functional types affect dissolved organic matter chemistry. *Plant and*
707 *Soil*, *407*(1), 135–143. https://doi.org/10.1007/s11104-015-2710-3
708 Roden, E. E., & Wetzel, R. G. (1996). Organic carbon oxidation and suppression of methane production
709 by microbial Fe(III) oxide reduction in vegetated and unvegetated freshwater wetland sediments.
710 *Limnology and Oceanography*, *41*(8), 1733–1748. https://doi.org/10.4319/lo.1996.41.8.1733

Saunois, M., Bousquet, P., Poulter, B., Peregon, A., Ciais, P., Canadell, J. G., Dlugokencky, E. J., Etiope, G., Bastviken, D., Houweling, S., Janssens-Maenhout, G., Tubiello, F. N., Castaldi, S., Jackson, R. B., Alexe, M., Arora, V. K., Beerling, D. J., Bergamaschi, P., Blake, D. R., … Peng, S. (2016). The global methane budget 2000-2012. *Earth System Science Data*, *8*(2), 697–751. http://dx.doi.org/10.5194/essd-8-697-2016

Schlesinger, W. H., & Bernhardt, E. S. (2020). *Biogeochemistry: An Analysis of Global Change* (4th ed.). Academic Press.

Segers, R. (1998). Methane production and methane consumption: A review of processes underlying wetland methane fluxes. *Biogeochemistry*, *41*(1), 23–51. https://doi.org/10.1023/A:1005929032764

Sihi, D., Inglett, P. W., Gerber, S., & Inglett, K. S. (2017). Rate of warming affects temperature sensitivity of anaerobic peat decomposition and greenhouse gas production. *Global Change Biology*, *24*(1), e259–e274. https://doi.org/10.1111/gcb.13839

Sorrell, B. K., Brix, H., Schierup, H.-H., & Lorenzen, B. (1997). Die-back of *Phragmites australis*: Influence on the distribution and rate of sediment methanogenesis. *Biogeochemistry*, *36*(2), 173–188. https://doi.org/10.1023/A:1005761609386

Stanley, E. H., & Ward, A. K. (2010). Effects of vascular plants on seasonal pore water carbon dynamics in a lotic wetland. *Wetlands*, *30*(5), 889–900. https://doi.org/10.1007/s13157-010-0087-x

Sutton-Grier, Ariana. E., Keller, J. K., Koch, R., Gilmour, C., & Megonigal, J. P. (2011). Electron donors and acceptors influence anaerobic soil organic matter mineralization in tidal marshes. *Soil Biology and Biochemistry*, *43*(7), 1576–1583. https://doi.org/10.1016/j.soilbio.2011.04.008

van Bodegom, P. M., & Stams, A. J. M. (1999). Effects of alternative electron acceptors and temperature on methanogenesis in rice paddy soils. *Chemosphere*, *39*(2), 167–182. https://doi.org/10.1016/S0045-6535(99)00101-0

van der Nat, F.-J., & Middelburg, J. J. (1998a). Effects of two common macrophytes on methane dynamics in freshwater sediments. *Biogeochemistry*, *43*(1), 79–104. https://doi.org/10.1023/A:1006076527187

van der Nat, F.-J. W. A., & Middelburg, J. J. (1998b). Seasonal variation in methane oxidation by the rhizosphere of *Phragmites australis* and *Scirpus lacustris*. *Aquatic Botany*, *61*(2), 95–110. https://doi.org/10.1016/S0304-3770(98)00072-2

van Hulzen, J. B., Segers, R., van Bodegom, P. M., & Leffelaar, P. A. (1999). Temperature effects on soil methane production: An explanation for observed variability. *Soil Biology and Biochemistry*, *31*(14), 1919–1929. https://doi.org/10.1016/S0038-0717(99)00109-1

Vann, C. D., & Megonigal, J. P. (2003). Elevated $CO_2$ and water depth regulation of methane emissions: Comparison of woody and non-woody wetland plant species. *Biogeochemistry*, *63*(2), 117–134. https://doi.org/10.1023/A:1023397032331

Waldo, N. B., Hunt, B. K., Fadely, E. C., Moran, J. J., & Neumann, R. B. (2019). Plant root exudates increase methane emissions through direct and indirect pathways. *Biogeochemistry*, *145*(1), 213–234. https://doi.org/10.1007/s10533-019-00600-6

Ward, S. E., Ostle, N. J., Oakley, S., Quirk, H., Henrys, P. A., & Bardgett, R. D. (2013). Warming effects on greenhouse gas fluxes in peatlands are modulated by vegetation composition. *Ecology Letters*, *16*(10), 1285–1293. https://doi.org/10.1111/ele.12167

Wassmann, R., Alberto, M. C., Tirol-Padre, A., Hoang, N. T., Romasanta, R., Centeno, C. A., & Sander, B. O. (2018). Increasing sensitivity of methane emission measurements in rice through deployment of 'closed chambers' at nighttime. *PLOS ONE*, *13*(2), e0191352. https://doi.org/10.1371/journal.pone.0191352

Weiss, J. V., Emerson, D., & Megonigal, J. P. (2004). Geochemical control of microbial Fe(III) reduction potential in wetlands: Comparison of the rhizosphere to non-rhizosphere soil. *FEMS Microbiology Ecology*, *48*(1), 89–100. https://doi.org/10.1016/j.femsec.2003.12.014

Weston, N. B., & Joye, S. B. (2005). Temperature-driven decoupling of key phases of organic matter degradation in marine sediments. *Proceedings of the National Academy of Sciences of the United States of America*, *102*(47), 17036–17040. https://doi.org/10.1073/pnas.0508798102

762 Whiticar, M. J. (1999). Carbon and hydrogen isotope systematics of bacterial formation and oxidation of
763 methane. *Chemical Geology*, *161*(1), 291–314. https://doi.org/10.1016/S0009-2541(99)00092-3
764 Wilson, R. M., Hopple, A. M., Tfaily, M. M., Sebestyen, S. D., Schadt, C. W., Pfeifer-Meister, L.,
765 Medvedeff, C., McFarlane, K. J., Kostka, J. E., Kolton, M., Kolka, R. K., Kluber, L. A., Keller, J. K.,
766 Guilderson, T. P., Griffiths, N. A., Chanton, J. P., Bridgham, S. D., & Hanson, P. J. (2016). Stability
767 of peatland carbon to rising temperatures. *Nature Communications*, *7*, ncomms13723.
768 https://doi.org/10.1038/ncomms13723
769 Yang, P., Wang, M. H., Lai, D. Y. F., Chun, K. P., Huang, J. F., Wan, S. A., Bastviken, D., & Tong, C.
770 (2019). Methane dynamics in an estuarine brackish *Cyperus malaccensis* marsh: Production and
771 porewater concentration in soils, and net emissions to the atmosphere over five years. *Geoderma*,
772 *337*, 132–142. https://doi.org/10.1016/j.geoderma.2018.09.019
773 Yang, Z., Wullschleger, S. D., Liang, L., Graham, D. E., & Gu, B. (2016). Effects of warming on the
774 degradation and production of low-molecular-weight labile organic carbon in an Arctic tundra soil.
775 *Soil Biology and Biochemistry*, *95*, 202–211. https://doi.org/10.1016/j.soilbio.2015.12.022
776 Ye, R., Jin, Q., Bohannan, B., Keller, J. K., & Bridgham, S. D. (2014). Homoacetogenesis: A potentially
777 underappreciated carbon pathway in peatlands. *Soil Biology and Biochemistry*, *68*(Supplement C),
778 385–391. https://doi.org/10.1016/j.soilbio.2013.10.020
779 Yvon-Durocher, G., Allen, A. P., Bastviken, D., Conrad, R., Gudasz, C., St-Pierre, A., Thanh-Duc, N., &
780 del Giorgio, P. A. (2014). Methane fluxes show consistent temperature dependence across microbial
781 to ecosystem scales. *Nature*, *507*(7493), 488–491. https://doi.org/10.1038/nature13164